3D finite element modeling of spiral welded pipe response to strike-slip fault

Mozhgan Asgarihajifirouz, Xiaoyu Dong, Hodjat Shiri
Department of Civil Engineering – Memorial University of Newfoundland, St. John's, Newfoundland, Canada

ABSTRACT
Spiral-welded pipelines are widely used for transferring the liquid and gas products. Permanent ground displacements (PGD) caused by fault crossing, landslides, and liquefactions may threaten the spiral-welded pipes and cause them to experience large strains well behind their elastic limits. Different helix angles of spiral welded pipelines generate different hoop and axial plastic strains. Therefore, the location of wrinkles and rotation demands change in the fault zone. In this paper, the seismic response of spiral-welded pipelines at strike-slip fault crossing was investigated using a dynamic explicit analysis to overcome the convergence issue that commonly occur in the analysis of post buckling problems. The helix angles and burial depth effects were evaluated on the nonlinear response of buried pipelines under various conditions, including different burial depths (shallow and deep) and intersection angles (perpendicular and inclined). The study showed the significance of helix angle and burial depth on the performance of spiral-welded pipelines and provide valuable insights for modeling the interaction between the spiral-welded pipelines and ground movements.

RÉSUMÉ
Les pipelines soudés en spirale sont largement utilisés pour le transfert des produits liquides et gazeux. Les déplacements permanents du sol (PGD) causés par le franchissement de failles, les glissements de terrain et les liquéfactions peuvent menacer les tuyaux soudés en spirale et leur faire subir de grandes contraintes bien en deçà de leurs limites élastiques. Différents angles d'hélice des pipelines soudés en spirale génèrent différentes déformations plastiques axiales et de cercle. Par conséquent, l'emplacement des rides et des exigences de rotation change dans la zone de faille. Dans cet article, la réponse sismique des pipelines soudés en spirale au croisement de failles décrochantes a été étudiée à l'aide d'une analyse explicite dynamique pour surmonter le problème de convergence qui se produit couramment dans l'analyse des problèmes de post-flambement. Les angles d'hélice et les effets de la profondeur d'enfouissement ont été évalués sur la réponse non linéaire des pipelines enterrés dans diverses conditions, y compris différentes profondeurs d'enfouissement (peu profondes et profondes) et angles d'intersection (perpendiculaires et inclinés). L'étude a montré l'importance de l'angle d'hélice et de la profondeur d'enfouissement sur les performances des pipelines soudés en spirale et fournit des informations précieuses pour la modélisation de l'interaction entre les pipelines soudés en spirale et les mouvements du sol.

1 INTRODUCTION

Welded steel pipelines are extensively used to transport oil, gas, and water from the source point to the consumption point. In recent years, the exploration and development of oil and gas have affected increasing demand for pipelines (seamless, UOE, spiral welded pipe), and according to TWI (The Welding Institute), the spiral-welded pipeline is 10-15% cheaper than UOE pipelines. Thus, the demand for producing the spiral-welded pipeline has increased.

Permanent ground deformations (PGD) caused by fault crossing, landslides, and liquefaction can destroy high-quality pipelines like spiral-welded pipelines that typically do not suffer damage caused by wave propagation.

Investigation of spiral-welded steel pipeline behavior under fault crossing is quite complex due to several events that may cause its failure. The number of research that evaluates the spiral-welded pipeline behavior is limited, but several attempts have been made to investigate the pipeline's behavior under fault movements.

In 1975, for the first time, Newmark and Hall investigated the buried pipeline behaviors affected by fault movement using a cable model. In this analysis, lateral soil strength and the flexural stiffness of pipelines were ignored. The Newmark and Hall idea was developed by adding soil lateral pressure, soil-pipe interaction, and pipe flexural stiffness in 1977. Kennedy et al. (1977) continued Newmark's work by considering the lateral strength of the soil, but still, they ignored the flexural stiffness of the pipe. The original work developed by Kennedy et al. (1977) was adopted by the ASCE guidelines (1984) for the design of buried pipelines. Development of the analytical methods was continued by Wang and Yeh (1985). In this study, the flexural stiffness of the pipeline is applied to the analytical model. Besides, the effects of soil-pipe lateral interaction and the large axial strains on pipeline bending stiffness are considered. Karamitros et al. (2011) proposed another analytical methodology that considered simple material nonlinearities and the second-order influences on the buried pipeline stress-strain analysis for the normal fault movement. These analytical solutions were developed for two-dimensional (2D) fault deformation, however; the fault movement is the three-dimensional (3D) problem and using a simplified stress-strain relationship may not represent the material response under large strain. In general, the analytical approaches are ideal for

understanding the behavior of pipeline generally because they cannot be implemented in problems with large fault movement or material nonlinearities.

The development of software and hardware technology in recent years has led to finite element analysis (FEA) has become more prevalent for investigating the nonlinear behavior of buried pipelines. Two different types of advanced numerical modeling techniques can be implemented to model soil and pipe interaction. The first one is the beam-spring model. In this modeling technique, the pipeline is discretized with beam elements, and spring elements model the soil. The second is the continuum model in which the soil has 3D solid finite elements, and the pipeline is modeled with shell elements. This model is implemented to overcome the limitations of the beam-spring model.

Liu et al. (2008) used a numerical model to simulate the pipe response under fault crossing. The pipe and soil interaction was modeled by soil-spring elements, and a shell finite element model was used to model the pipelines crossing the active fault zone. As presented in this study, the fault movement creates localized axial strain at the early stage of loading, and the localized strain location depends on the loading fault mode.

O'Rourke et al. (2009) and Xie et al. (2011) investigated the polyethylene pipeline mechanical behaviors under fault crossing in different soil conditions. In this research, they assessed the direct influence of increasing soil stiffness and the interaction between soil and pipe and pipe stress.

Vazouras et al. (2012) assessed the effects of boundary conditions on pipeline responses. They investigated two pipes with limited and unlimited ends subjected to different tensile loads. The results show that the pipes exhibit local strain when the fault displacement rate is low. As the fault displacement rate increases, ovalization phenomena occur in the local strain spot.

Zhang et al. (2015; 2016) used the finite element method to investigate the buckling behavior of buried pipelines. It has been founded that fault displacement slightly impacted the buried pipeline's maximum strain location. Besides, as the thickness of the wall increases, the buried pipeline's deformation curve becomes smoother.

The influence of ground movement on the buried pipelines crossing strike-slip fault has been investigated by Vazouras et al. (2015) considering different fault angles. Besides, in this study, the critical fault offset was evaluated based on different performance criteria.

Jalali et al. (2016) have conducted experimental and finite element studies on the reverse faulting effects on buried gas pipelines. The results represent the dependency of uplift force to the pipe diameter and its relative stiffness, while the ALA proposed a constant force for the burial depth.

Kaya et al. (2017) assessed the spiral-welded pipeline behavior at the Kullar fault movement. In this paper, the effects of boundary conditions have been investigated. The 3D nonlinear continuum model has been used to model the interaction between the soil and pipeline by considering internal pressure. The soil axial resistance was modeled by equivalent springs at the pipeline end. The results show that the pipe behaviors under compressive strain are very sensitive to the end boundary conditions, soil properties, and internal pressure.

The present work investigates the nonlinear behavior of buried spiral-welded pipelines to the strike-slip fault under various conditions, including different burial depths and helical angles. The significance of the helix angles effect on the behavior of the spiral-welded pipeline provides valuable insights to the design of this kind of pipeline in the fault zone.

2 NUMERICAL MODEL

Several welded steel pipelines were subjected to fault offset in the 1999 Kocaeli earthquake. The main water transmission pipeline was a 2.20 m diameter spiral-welded pipeline that experienced significant damage and leaked due to a rupture of the right-lateral offset of the North Anatolian fault. This pipeline had been installed just a year prior to the earthquake and crossed the fault with an angle of 55°. Consequently, the pipeline suffered one minor and two major wrinkles. In this study, the response of Thames water transmission is used to verify the 3D nonlinear continuum model. The structural response of the spiral-welded pipeline to the strike-slip fault is investigated numerically by utilizing advanced computational tools. The general-purpose finite element (FE) program, ABAQUS, is employed to compute the nonlinear response of the steel pipeline.

The schematic diagram of the buried spiral welded pipeline, which was supposed to the strike-slip fault rupture, is presented in Figure 1. It illustrates that these kinds of pipelines suffer from local buckling, cross-sectional distortion, and tensile and compressive strains when subjected to strike-slip fault rupture. Figure 2 represents the trench cross-section in the FE model. As shown in this figure, the depth and width of the trench are 5.0 m and 20.0 m, respectively. In this study, the diameter, thickness, and length of the pipeline are 2.20 m, 0.018 m, and 100.0 m, respectively.

To model the soil domain, eight-node linear brick reduced integration hour-glassing control elements (type C3D8R) were used. Besides, four-node reduced integration shell elements (type S4R) were used for modeling the cylindrical pipeline. In this study, to reduce the computational time, the mesh size increases toward the boundaries in the soil elements.

The steel pipeline was API Grade B with the minimum specified yield stress of 241 MPa. An elastic-perfectly plastic Mohr-Coulomb model is considered for the soil behavior, characterized by the soil cohesiveness c, the friction angle φ, the elastic modulus E, and Poisson's ratio ν. The dilation angle ψ is assumed to be equal to zero through this study. Table 1 gives the properties of steel pipeline. The backfill material of the trench was non-homogenous soil. It is a mixture of native soil (soft and stiff clay) with sand and gravel. The soil properties are presented in Table 2. One of the significant hurdles was the lack of information regarding material properties in the published paper. However, the results are in good agreement with the numerical study conducted by Kaya et al. (2017).

A surface-to-surface contact algorithm is considered between the outer face of the steel pipeline and the surrounding soil. The model allows separation between surfaces after contact occurs. The friction coefficient between the surfaces is taken to be $\mu = 0.3$.

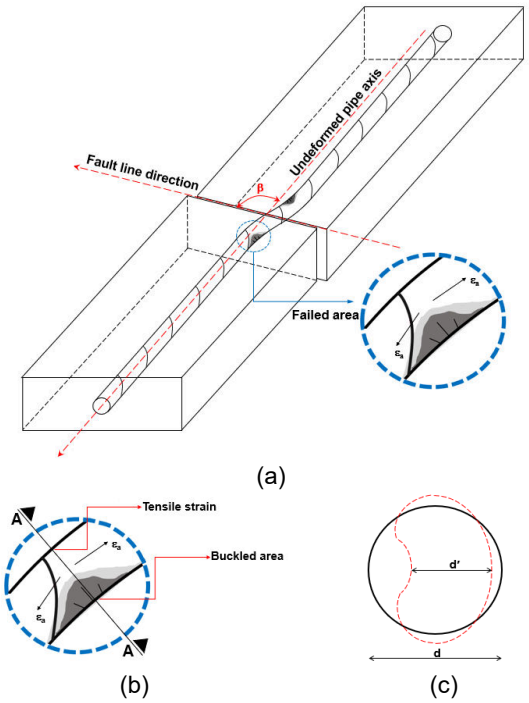

Figure 1. Schematic representation of a pipeline interaction with strike-slip fault rupture; (a) deformed shape, (b) failed area, (c) ovalization parameter definition.

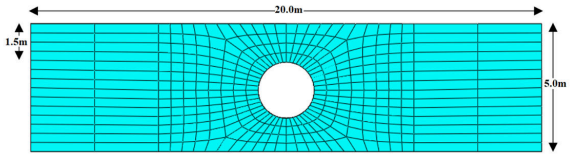

Figure 2. The FE model and cross-sectional view of the soil (Kaya et al. (2017)).

Table 1. Steel pipeline properties.

Min Yield stress (MPa)	Min Tensile stress (MPa)	Young Modulus (GPa)	Min yield strain	Elongation (%)
241	414	210	0.002	23

Table 2. Soil properties.

Soil type	Cohesion (kPa)	Young Modulus (MPa)
Soft	20	8
Stiff	40	16

The quasi-static nonlinear analysis of soil and pipe systems was performed in three separate steps: First, gravity loading was applied. In the second step, the internal pressure of 10 bar was applied, and in the third, the incremental fault displacements were applied.

3 RESULTS

3.1 Verification basis

The 3D fixed boundary condition model from numerical studies of Kaya et. al (2017) is used to verify the FE model. The geometry of model and the mechanical properties of material are presented in the previous section.

Based on the May 2001 Eidinger Report, the distance between the two major wrinkles was 17.1 m. The numerical analysis conducted by Kaya et al. (2017), shows that the distance between these two wrinkles is 16.5 m when the fault displacement is 1.0 m and fixed boundary condition are considered to do the analysis. The verified model results are presented in Figure 3 and Table 3. Figure 3 shows the deformed shapes of pipeline in the verified model. In this model, the distance between two major wrinkles is 16.51 m. Table 3 represents a comparison between the numerical study conducted by Kaya et al. (2017), field observation and the verified model. As shown in Table 3, there is good correlation between the verified model, field observation and the previous numerical analysis.

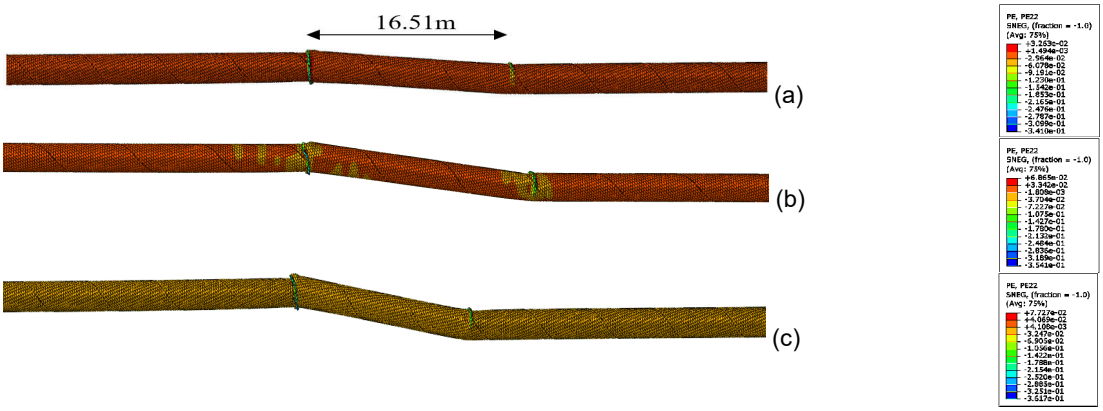

Figure 3. Deformed shapes of pipe (w/ internal pressure) and separation distance of wrinkles at fault displacements of (a) 1.0, (b) 2.0, and (c) 3.0 m (fixed end BC) of the verified model.

Table 3. Comparison of verified numerical model results with field observations and the numerical model conducted by Kaya et al. (2017).

	Separation distance between wrinkles (m)	Average axial strain at wrinkles (1&2)	Rotation demands at wrinkles (1& 2) (degrees)	Location of the 3rd minor wrinkle (m)	Local buckling wavelength (cm)	Local buckling strain (%)
Field observation	17.1-17.6	15-20%	7.5-8.5°	13.0	50-60	-
Kaya et al. (2017)	16.5	15-20%	7.5-8.0°	13.1	50-55	0.21
Verified model	16.51	15-20%	7.1-8.9°	13.3	50-55	0.22

3.2 Parametric studies

3.2.1 Effect of burial depth

The responses of spiral-welded pipeline to the strike-slip fault considering two different burial depths (1.50 and 3.0 m) is evaluated in this section. Figure 4 shows the distribution of axial strain versus fault displacements. It should be noted that Wrinkle 1 is a wrinkle in the stiff soil and Wrinkle 2 is in the soft soil. As shown in this figure, as the burial depth increases, the maximum axial strain increases in the wrinkles. When the burial depth increases, the weight of soil and cohesive forces increase. Therefore, the buried pipeline in the deep depth fails earlier than the buried pipeline in the shallow depth. The deformed shapes of the pipeline at the different burial depths are presented in Figure 5.

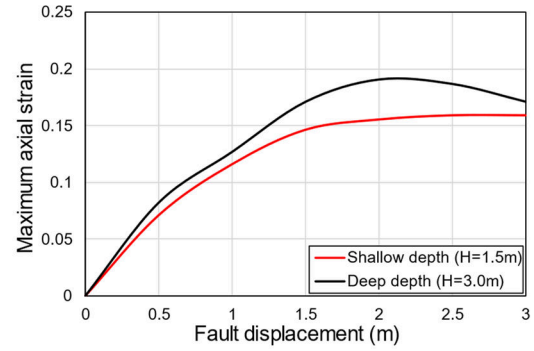

(a)

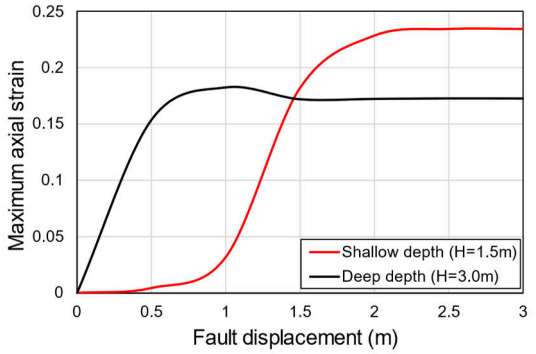

(b)

Figure 4. Effect of burial depth on the maximum axial strain, (a) Wrinkle1, (b) Wrinkle2.

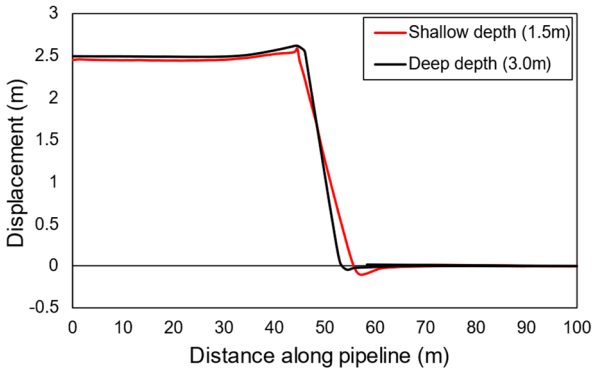

Figure 5. Deformed shapes of pipeline in the shallow depth (1.5 m) and the deep depth (3.0 m).

3.2.2 Effect of helix angle

In this section, the effect of helix angle on the pipeline response considering different burial depths is investigated. Figure 6 represents the effect of different helix angles on the deformed shape of the spiral-welded pipeline. As shown in these figures, the distance between the wrinkles is decreased as the burial depth increases. Besides, depending on the helix angles, the distance between two major wrinkles changes. The distance between the wrinkles is presented in Table 4.

In the shallow depth, the helix angle of 40° creates a long distance, while in the deep depth, the helix angle of 45° creates a larger distance value between two major wrinkles.

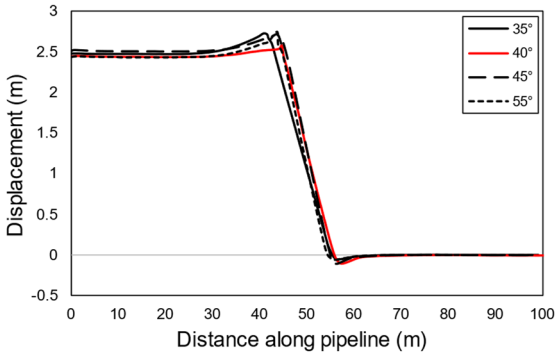

(a)

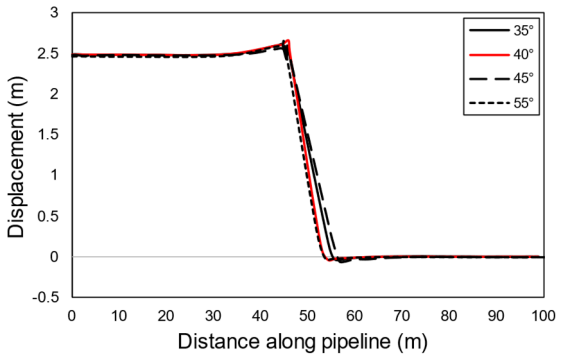

(b)

Figure 6. Deformed shapes of pipeline considering different helix angle in (a) shallow depth (1.5 m), (b) deep depth (3.0 m).

The finite element results have been presented in Table 4. The presented results in this table illustrate the significance of the helix angle effect on the response of the spiral-welded pipeline to the strike-slip fault.

The distribution of axial strain of the spiral-welded pipelines have been presented in Figure 7. As shown in this figure, the ovalization and shape of wrinkles change as the helix angle changes.

The comparison between results of different helix angles in Table 4 shows that in the shallow depth, the helix angle of 40° produces the lowest ovalization parameter. Besides, the ovalization parameter of the spiral-welded pipeline with the helix angle of 45° buried in the deep depth is the lowest value. It means that as the distance between the fault line and the location of wrinkle increases, the amount of ovalization parameter decreases.

Table 4. Finite element results for different burial depth and helix angle.

Burial depth	Helix angle (°)	Separation distance between wrinkles (m)	Average axial strain at wrinkles (1&2)	Ovalization parameter	Location of the 3rd minor wrinkle (m)
Shallow depth (1.5m)	35	14.90	10-19%	0.09	-
	40	16.51	15-20%	0.07	13.30
	45	12.02	17-21%	0.11	9.36
	55	11.89	18-22%	0.13	8.61
Deep depth (3.0m)	35	10.62	12-20%	0.13	3.74
	40	8.94	16-23%	0.15	-
	45	11.65	13-22%	0.08	-
	55	8.66	19-24%	0.16	4.30

The tensile rupture strain capacity of modern pipelines with high-quality welding is presented in the American Lifelines Alliance (ALA) guidelines and Pipeline Research Council International (PRCI) for gas and liquid hydrocarbon pipelines. The tensile strain limit of pipelines where the performance target is to preserve pressure integrity is 4% and 2-4% in the ALA and PRCI guidelines. If the performance target is immediate serviceability, such as post-event functionality, the ALA strain limit is 2%, while the PRCI limit is 1-2%. The comparison of the average axial strain at the wrinkles with these limit states in Table 4 shows that the induced strain at the wrinkles is far beyond the limitations of ALA or PRCI codes. Thus, these pipelines failed at this fault displacement (3.0 m).

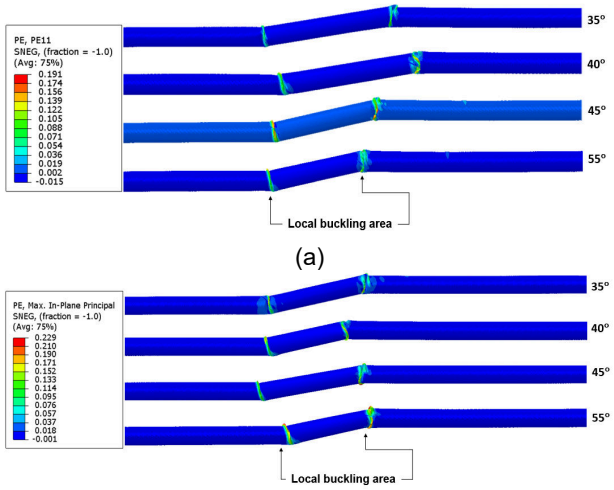

Figure 7. Strain distribution along the pipeline considering different helix angle in (a) shallow depth (1.5 m), (b) deep depth (3.0 m).

4 CONCLUSION

The results represent that the helix angle of the spiral-welded pipeline has an influence on the location of local buckling. The helix angle of the spiral-welded pipeline is an important factor that affects the reduction of axial strain and deformation of the pipeline. Therefore, considering a suitable helix angle for a pipeline is recommended when passing a pipe through a fault line is inevitable.

5 ACKNOWLEDGEMENT

The authors gratefully acknowledge the financial support of the “Wood” through establishing Research Chair program in Arctic and Harsh Environment Engineering at the Memorial University of Newfoundland, the “Natural Science and Engineering Research Council of Canada (NSERC)” and the “Newfoundland Research and Development Corporation (RDC) (now InnovateNL) through “Collaborative Research and Developments Grants (CRD)”. Special thanks are extended to Memorial University for providing excellent resources for conducting this research program.

6 REFERENCES

Abdoun, T. H., Ha, D., O’Rourke, M. J., Symans, M. D., O’Rourke, T. D., Palmer, M. C., & Stewart, H. E. (2009). Factors influencing the behavior of buried pipelines subjected to earthquake faulting. *Soil Dynamics and Earthquake Engineering*, 29(3), 415-427.

ALA, 2005. American Lifelines Alliance Guidelines for the Design of Buried Steel Pipes.

American Society of Civil Engineers, 1984. *Guidelines for the Seismic Design of Oil and Gas Pipeline Systems*, D. J. Nyman (editor).

Jalali, H. H., Rofooei, F. R., Attari, N. K. A., & Samadian, M. (2016). Experimental and finite element study of the reverse faulting effects on buried continuous steel gas pipelines. *Soil Dynamics and Earthquake Engineering*, 86, 1-14.

Karamitros, D. K., Bouckovalas, G. D., Kouretzis, G. P., & Gkesouli, V. (2011). An analytical method for strength verification of buried steel pipelines at normal fault crossings. *Soil Dynamics and Earthquake Engineering*, 31(11), 1452-1464.

Kaya, E. S., Uckan, E., O'Rourke, M. J., Karamanos, S. A., Akbas, B., Cakir, F., & Cheng, Y. (2017). Failure analysis of a welded steel pipe at Kullar fault crossing. *Engineering Failure Analysis*, 71, 43-62.

Kennedy, R. P., Williamson, R. A., & Chow, A. M. (1977). Fault movement effects on buried oil pipeline. *Transportation Engineering Journal of ASCE*, 103(5), 617-633.

Liu, X., Zhang, H., Wu, K., Xia, M., Chen, Y., & Li, M. (2017). Buckling failure mode analysis of buried X80 steel gas pipeline under reverse fault displacement. *Engineering failure analysis*, 77, 50-64.

Newmark, N. M., & Hall, W. J. (1975, June). Pipeline design to resist large fault displacement. In *Proceedings of US national conference on earthquake engineering* (Vol. 1975, pp. 416-425).

PRCI. (2009). Guidelines for constructing natural gas and liquid hydrocarbon pipelines through areas prone to landslide and subsidence hazards.

Vazouras, P., Karamanos, S. A., & Dakoulas, P. (2012). Mechanical behavior of buried steel pipes crossing active strike-slip faults. *Soil Dynamics and Earthquake Engineering*, 41, 164-180.

Vazouras, P., Dakoulas, P., & Karamanos, S. A. (2015). Pipe–soil interaction and pipeline performance under strike–slip fault movements. *Soil Dynamics and Earthquake Engineering*, 72, 48-65.

Wang, L. R. L., & Yeh, Y. H. (1985). A refined seismic analysis and design of buried pipeline for fault movement. *Earthquake engineering & structural dynamics*, 13(1), 75-96.

Xie, X., Symans, M. D., O'Rourke, M. J., Abdoun, T. H., O'Rourke, T. D., Palmer, M. C., & Stewart, H. E. (2011). Numerical modeling of buried HDPE pipelines subjected to strike-slip faulting. *Journal of Earthquake Engineering*, 15(8), 1273-1296.

Zhang, J., Liang, Z., Han, C. J., & Zhang, H. (2015). Numerical simulation of buckling behavior of the buried steel pipeline under reverse fault displacement. *Mechanical Sciences*, 6(2), 203-210.

Zhang, J., Liang, Z., & Zhang, H. (2016). Response analysis of buried pipeline subjected to reverse fault displacement in rock stratum. *Transactions of FAMENA*, 40(3), 91-100.